

Characteristics of Bacterial Pumps in Microfluidic Systems

MinJun Kim and Kenneth S. Breuer*

*Division of Engineering, Box D, Brown University, Providence, RI 02912, USA, kbreuer@brown.edu

ABSTRACT

We demonstrate that flow-deposition of bacteria can successfully create a live bacterial carpet which can generate local fluid motion inside a micro-fabricated system. The carpet-activated microfluidic system can be used not only to enhance mixing but also to pump fluid autonomously for several hours. The mixing and pumping performance of the system changes in response to modifications to the chemical and thermal environment of the bacteria. The mixing performance, measured by tracking the dispersion of small particles can be increased by the addition of glucose (food) to the surrounding buffer, or by increasing the flagellar motor activity by raising the buffer temperature. Increasing the glucose concentration also results in an increase of the maximum pumping velocity, presumably due to increased cellular activity. In addition, the pumping performance is affected by the global geometry of the pump with narrower channels achieving a higher pumping velocity at an earlier time after the carpet creation.

Keywords: *Serratia marcescens*, microfluidics, mixing, pumping, bacterial carpet, motility, decay rate.

1 INTRODUCTION

Due to the difficulty in fabricating nano-scale motors and developing micron-scale power sources, the pumping of fluids in microfluidic systems is currently achieved by relatively large external actuators such as syringe pumps, or high voltage power supplies. Although these devices are effective, they are cumbersome and inefficient, often dominating in size and power consumption over the microfluidic network to which they are connected. An alternative approach of manipulating fluids moving efficiently in microfluidic networks is to utilize the bio-molecular motors from flagellated bacteria such as *E.coli* or *Serratia marcescens* as fluidic actuators [1,2], using external stimuli such as temperature [3], chemical concentration gradients [4], and geometrically restrictive environments [5] to control and direct bacterial behavior.

When wide-type *Serratia marcescens* are patterned onto the surface of a microchannel in a dense-packed manner, they form a bacterial carpet [2] in which the flagellar motion enhances the effective diffusion of tracer particles [2]. The properties of this “bacterial carpet” with their flagella oriented in one direction can not only pump fluid as a plug-like flow [6] but also transport PDMS chips through a fluid medium [2]. It is advantageous for microfluidic networks to use the bacterial motor system in that the

bacteria draw their propulsion energy (protons) from the nutrients in the motile buffer [2, 7] and hence the system requires no external components for operation.

Flagellated bacteria are exquisitely sensitive to a wide variety of external stimuli. They respond to thermal and chemical gradients which directly influence their motive characteristics and form the basis for chemotactic and thermostatic responses [1]. Changes in factors such as temperature, the concentration of certain sugars, or the spatial environment can stimulate the bacteria's sensory pathway and hence affect aspects of their motor performance, including the counterclockwise and clockwise rotation intervals and the rotation frequency [3,4,5]. The present paper explores the use of external stimuli to affect the global performance of bacterial mixers and pumps and demonstrates that we can use both geometric and environmental factors to control and enhance the level of useful work achieved by the device.

2 FORMATION OF BACTERIAL CARPETS

Robust bacterial carpets were formed on the inner surfaces of a microfluidic channel using a flow deposition procedure [6]. Microchannels measuring $200\ \mu\text{m}$ (W) \times $15\ \mu\text{m}$ (D) \times $15\ \text{mm}$ (L) were fabricated from PDMS using standard soft-lithographic techniques [8]. Using a syringe pump, a buffer containing a high concentration ($2 - 5 \times 10^9/\text{ml}$) of motile *Serratia marcescens* was pumped through the channel at a low flow rate ($0.05\ \mu\text{l}/\text{min}$). After five seconds, the pump was switched off, and the system was allowed to settle for five minutes. During this time, the bacteria swim randomly through the channel, sticking on contact to bare spots on the PDMS and glass surfaces. The flow-and-settle cycle was repeated until the surface was coated to the desired density. To counteract gravitational sedimentation effects, the system must be rotated to ensure an even coating of all surfaces. The formation of the carpet was tracked optically using Differential Interference Contrast (DIC) microscopy.

The density of the bacterial carpet and the orientation of the cells were measured during and after the carpet deposition process. The DIC image was pre-processed by removing the static background image and then thresholding to enhance the outline of each cell body (Figure 1). MATLAB-based image processing tools were used to determine the cell density (“fill factor”) and distributions of the cell orientation. The most probable orientation of the cells was observed to be parallel to the major axis (x) of the channel, and it was found that 60% of

the cells were aligned between - 30 and 30 degrees with respect to the channel's x -axis. After 3000 sec, the fill factor was measured to be 83% ($\pm 1.2\%$) and the average density of bacteria was 31.3 /100 μm^2 (± 2.1).

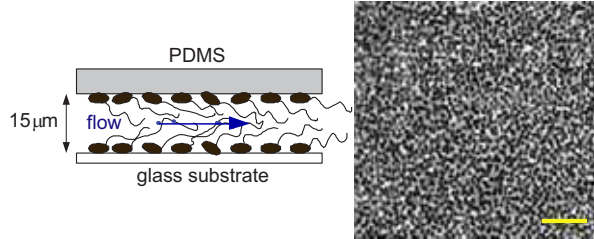


Figure 1: Schematic of the bacterial pumping system and micrograph of the bacterial carpet as it develops inside the microfluidic system. The picture is taken 2000 seconds after the initiation of the flow deposition procedure. The scale bar is 10 μm .

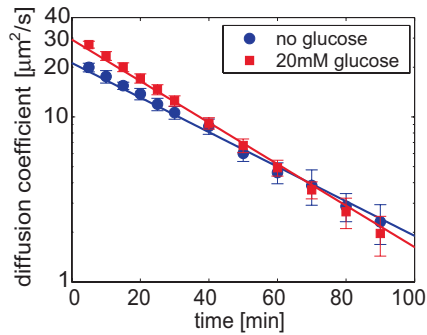


Figure 2: Enhancement of particle Diffusion coefficient D as a function of time. The diffusion due to Brownian motion has been subtracted

3 MIXING ENHANCEMENTS IN A SEALED SYSTEM

Following the formation of the carpet, the external flow was switched off and the inlet and outlet tubes sealed using RTV silicone adhesive sealant. The motion of fluorescent particles (490 nm dia.) suspended in the ambient buffer solution was measured using standard fluorescence microscopy techniques. Several image-pairs, each pair consisting of two CCD images (5 ms exposure, separated by 50 ms) were acquired. Particle displacement between the two images was computed using a custom particle tracking velocimetry (PTV) algorithm written using MATLAB. Velocity vectors were then calculated from each displacement vector. Typically 100 images pairs were recorded at a fixed point in the channel over the course of few minutes. Approximately 3000 velocity vectors were computed at each condition. Using a 100 \times objective lens, the image resolution is 67 nm/pixel, and assuming a tracking accuracy of 0.05 pixels, the velocity resolution is 67 nm/s.

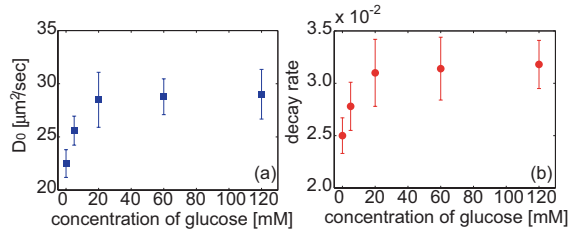


Figure 3: Variation of the initial diffusion coefficient (a) and the decay rate (b) of bacterial carpets in response to changes in concentration of glucose (0, 2, 20, 60, 120 mM).

3.1 Effects of Glucose Concentration

Immediately after the carpet creation, beads were observed to move rapidly, and over long distance. In contrast, the bead motion was much more subdued long times (hours) after the carpet creation. Particle displacement statistics were acquired at several times following the carpet formation. The motion was characterized by computing an effective diffusion coefficient, D_p , from the mean-square particle displacement statistics. D_p was observed (figure 2) to have its maximum value, D_0 immediately after the carpet's formation, after which time it decays exponentially, with a decay rate α , asymptoting towards a constant value, D_b , governed by thermal (Brownian) motion [2]:

$$D_p = D_0 \exp(-\alpha t) + D_b \quad (1)$$

These measurements were repeated for a variety of conditions, two of which are shown in Figure 2, from which we see that the elevated glucose concentration serves to increase the initial diffusion coefficient, but also to increase the decay rate. Figure 3 shows the dependence of the initial diffusion coefficient and the decay rate of the particle diffusion due to bacterial carpets in response to changes in concentration of glucose. A slight increase in the buffer glucose concentration quickly increases the initial diffusion coefficient, although as the concentration increases the diffusion coefficient approaches a plateau. This behavior is due to the fact that, although the presence of small concentrations of glucose does increase the metabolic rate of the bacteria, resulting in higher motor rotation rates [7,9], the glucose consumption rate per cell quickly saturates at a buffer concentration of approximately 20 mM above which the increased concentration has no additional effect. The same behavior is seen with the decay rate of the diffusion coefficient. This may be explained by the fact that bacterial catabolism (destructive metabolism) of glucose rapidly produces lactic, acetic, citric, and pyruvic acids in the buffer [10], and since the system is sealed, there is no mechanism to remove these waste products and they cause the buffer pH to drop. Cellular activity, including motor motion is driven by trans-membrane pH gradient and

significantly influences the rotation of bacterial flagellum [7] and as the pH drops, the cell motility (and thus the carpet motility) falls [1]. Thus in these sealed systems, the carpets activity directly leads to its own decline and at the elevated metabolic rates induced by the superabundant glucose concentrations, this process is only made more extreme.

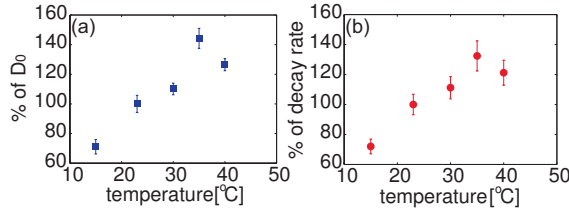


Figure 4: Variation of the initial diffusion coefficient (a) and the decay rate (b) due to bacterial carpet motility as a function of temperatures. The increase in temperature of a buffer shows an increase in the initial motility and a increase in the decay rate up to 35 °C.

3.2 Effects of Temperature

The flagellar motion on the bacterial carpet is also quite sensitive to temperature because an individual bacteria's motility pattern is determined by the frequency of tumbling and rotation [3,9]. Using the procedure described above, the evolution of the effective diffusion coefficients as a function of time were measured at different ambient temperatures. The percentage deviation from the baseline measurement (at 23°C) of the initial diffusion coefficient, D_0 , and the decay rate, α , is shown in figure 4.

In general, the initial diffusion coefficient increases with increasing temperature until it reaches a peak at 35 °C. The dip at 40 °C might be related to the fall in the tumbling frequency at higher temperatures [3] which may lead to reduced hydrodynamic effectiveness. This needs to be studied further. As with the glucose dependence, the behavior of the diffusion coefficient decay rate follows closely the behavior of the initial diffusion coefficient and strengthens the hypothesis that the reduction in carpet effectiveness is directly caused by the production of metabolic side-products, and that at higher metabolic rates (due to glucose or temperature effects), higher carpet activity is accompanied by a faster decline in motility.

4 ENHANCEMENT OF PUMPING PERFORMANCE

If the inlet and outlet ports of the microchannel are not sealed, we observe that the bacterial carpet self-organizes and starts to pump fluid through the channel in a self-sustained manner [6]. The fluid moves through the channel with a uniform plug flow, driven by the “slip velocity” generated by the carpet on the channel wall. Figure 5 shows evolution of the average flow velocity as a function of the

time following the creation of the carpet-coated microchannel. We see that the velocity grows linearly for a short time before it reaches a maximum at $t = t^*$, after which time it begins to decay. We can thus characterize the performance of the bacterial pump as being comprised of two phases: a period of linear growth (red line):

$$u = \varphi t \quad (t < t^*) \quad (2)$$

Where φ is the growth rate, followed by a period of exponential decay (blue line):

$$u = u_{\max} \exp[-\zeta(t-t^*)] \quad (t > t^*) \quad (3)$$

where ζ is the decay rate.

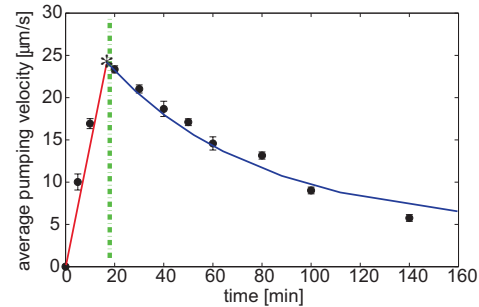


Figure 5: Evolution of the average flow velocity generated by the bacterial pump (no external stimuli). The flow reaches a maximum approximately 20 minutes after the carpets creation and then decays.

4.1 Effects of Glucose Concentration

The performance of the pump, as define by the maximum pumping velocity, the time to maximum performance and the velocity decay rate, was characterized as a function of the concentration of glucose in the buffer solution. As shown in Fig. 6, maximum pumping velocities are significantly enhanced by increases in the glucose concentration in the motile buffer. As before, the performance increases do tend to saturate, although the concentration at which the saturation occurs appears to be higher than was the case for the sealed system. This is likely due to the fact that, since fresh buffer is continuously entering the system, and since waste products are continually being pumped out of the system, the exposure of an individual cell to the products of catabolism are reduced and hence the carpet is more resilient to the effects of its own activity. The time at which the peak velocity is reached (t^*) is not affected by the glucose concentration (remaining constant at approximately 16.5 min) suggesting that the enhanced flagellar motion does not result in faster self-organization and that this global coordination has little to do with the local cellular processes, but more to do with the overall structure of the carpet.

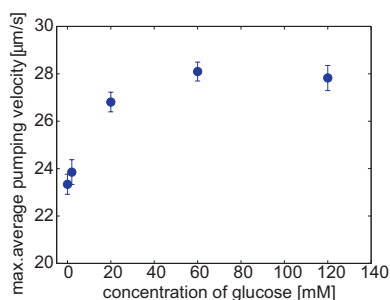


Figure 6: Variation of the maximum pumping velocity as a function of glucose concentration (0, 2, 20, 60, 120 mM).

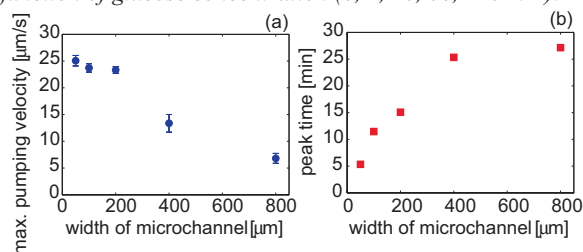


Figure 7: Variation of the maximum pumping velocity (a) and its peak time (b) as a function of width of channel. Wider channels achieve lower pumping speeds, presumably due to poorer global coordination at such large scales.

4.2 Effects of Pump Geometry

The geometry of the microchannel will affect the performance of the bacterial pump in two ways. Firstly, it is known that the behavior and motion of bacteria can be influenced by their geometric environment [5, 12]. Secondly, even if the bacterial behavior remains unchanged, the self-organization of the carpet may be a function of the pump geometry. The results shown thus far were performed in a microchannel measuring 15 µm deep 200 µm wide and 15 mm long. Figure 7 shows the maximum pumping velocity and the time to maximum pumping, t^* , as a function of the channel width (keeping the length and depth constant). Five channel widths were tested: $w = 50, 100, 200, 400,$ and 800 µm. The results are quite striking, and we see that both the maximum pumping velocity achieved and the time to peak performance are strongly affected by the channel width with improved performance achieved with narrow channels. For the 50 µm channel, a maximum speed of 25 µm/s is achieved immediately after the channel is created (to within our ability to measure), while the widest channel tested, $w = 800$ µm, barely pumps at all and requires over 25 minutes to reach its best performance. Since we assume that the individual cell behavior is not affected by the pump geometry, we can only conclude that the geometry affects to nature of the flagellar coordination that leads to the global pumping behavior, and that the narrower channels coordinate faster and with more efficiency leading to the observed global pumping performance. Decreasing the pump length also increased

the maximum pumping speed and decreased t^* , however the effects were moderate (improvements of approximately 10% for a three-fold reduction in channel length).

5 CONCLUSIONS

The performance of microfluidic devices powered by bacterial carpets has been shown to be a sensitive function of both the environment in which the bacteria live as well as the global device geometry. Factors that enhance bacterial motility, such as the concentration of glucose and the system temperature, similarly affect the carpet motility and hence the overall particle diffusion (mixing) and transport (pumping). The decline of the device performance is thought to be related to the effects of catabolism in which by-products of the carpet metabolism reduces the buffer pH and hence leads to a reduction in motility and device performance. Other chemical effects will also influence pump performance. Most importantly the role of dissolved oxygen will need to be explored, although simple calculations suggest that there is more than enough oxygen in the standard buffers to support the carpets over the few hours that each experiment lasts. Perhaps the most intriguing result, is the finding that the geometry of the pump, specifically the channel width, affects its global performance dramatically, and that in the narrow channels, where coordination is achieved almost immediately, the pumping velocity approaches a maximum speed that is comparable to that achieved by freely-swimming cell.

This work was supported by the DARPA BioMotors program. The assistance and collaboration with Howard Berg, Linda Turner, Nicholas Darnton, Tom Powers, Greg Huber and MunJu Kim are most gratefully acknowledged

REFERENCES

- [1] H. C. Berg, *Annu. Rev. Biochem.*, 72, 19, 2003.
- [2] N. Darnton, L. Turner, K. Breuer, and H. C. Berg, *Biophysical J.*, 86, 1863, 2004.
- [3] K. Maeda, Y. Imae, J. -I. Shioi, and F. Oosawa, *J. Bacteriol.*, 127, 1039, 1976.
- [4] R. M. Macnab, and R. M. Koshland, *Proc. Natl. Acad. Sci. USA*, 69, 2509, 1972.
- [5] H. C. Berg, and L. Turner, *Biophysical J.*, 58, 919, 1990.
- [6] M. J. Kim, and K. S. Breuer, in preparation, 2005.
- [7] M. D. Manson, P. Tedesco, H. C. Berg, F. M. Harold, and C. Van Der Drift, *Proc. Natl. Acad. Sci. USA*, 74, 3060, 1977.
- [8] G. Whitesides, and A. Strooks, *Phys. Today*, 54 (6), 42, 2001.
- [9] D. F. Blair, *Nanotechnology*, 2, 123, 1991.
- [10] M. Solé, N. Rius, and J. G. Lorén, *Internatl Microbiol.*, 3, 39, 2000.
- [11] J. M. Janda, and S. L. Abbott, "The Enterobacteria," Lippincott-Raven Publisher, 1998.
- [12] Z. Liu, and K. D. Papadopoulos, *Appl. Environ. Microbiol.*, 61, 3567, 1995.